Volume 1 | Number 1 | Jan 2013 | Pages 1–100

JAAS

Journal of Analytical Atomic Spectrometry
www.rsc.org/jaas

Hg

Pb

Fe

ROYAL SOCIETY OF CHEMISTRY

This is an *Accepted Manuscript*, which has been through the Royal Society of Chemistry peer review process and has been accepted for publication.

Accepted Manuscripts are published online shortly after acceptance, before technical editing, formatting and proof reading. Using this free service, authors can make their results available to the community, in citable form, before we publish the edited article. We will replace this *Accepted Manuscript* with the edited and formatted *Advance Article* as soon as it is available.

You can find more information about *Accepted Manuscripts* in the **Information for Authors**.

Please note that technical editing may introduce minor changes to the text and/or graphics, which may alter content. The journal's standard **Terms & Conditions** and the **Ethical guidelines** still apply. In no event shall the Royal Society of Chemistry be held responsible for any errors or omissions in this *Accepted Manuscript* or any consequences arising from the use of any information it contains.

Femtosecond and Nanosecond LIBS Studies of Nitroimidazoles: Correlation between Molecular Structure and LIBS data

E. Nageswara Rao,[a] P. Mathi,[b,#] S. Abdul Kalam,[a] S. Sreedhar,[a] Ajay K. Singh,[b] B.N. Jagatap,[c] and S. Venugopal Rao[a,*]

[a]*Advanced Centre of Research in High Energy Materials (**ACRHEM**), University of Hyderabad, Prof. C. R. Rao Road, Gachibowli, Hyderabad 500046, Telangana, India.*

[b]*Radiation & Photochemistry Division, [c]Chemistry Group Bhabha Atomic Research Centre (BARC), Mumbai 400 085, India.*

Abstract

In the present study, seven novel explosive molecules (nitroimidazoles) have been investigated for laser induced breakdown (LIB) spectral signatures of molecular and atomic species in air and argon atmospheres utilizing both femtosecond (fs) and nanosecond (ns) laser pulse excitation. The molecular emissions were observed to be stronger in the fs spectra whereas atomic emissions were prominent in the ns spectra recorded in both air and argon atmospheres. The C_2 Swan band was strongest in argon atmosphere while CN violet band was strongest in ambient environment. The LIB spectra were analysed for understanding (a) the influence of molecular structure i.e. type of bonds (C-C, C=C, C-N and C=N) on atomic (C, H, N and O) and molecular (CN, C_2 and NH) emissions, (b) effect of surrounding atmosphere on the fs and ns LIB spectra, (c) correlation between stoichiometric and intensity ratios of molecular as well as atomic species, (d) effect of the number of substituents and their position in the ring on the fragmentation pathways and (e) correlation between oxygen balance and LIB spectra. Furthermore, time resolved spectroscopic studies of the plasma induced by fs and

1   ns laser pulses have been carried out to understand the temporal evolution and possible

2   reaction mechanisms of various molecular species. An attempt has been made to correlate the

3   spectral emission with the chemical structure for this series of energetic materials. Our

4   detailed studies and analyses clearly suggest that atomization/fragmentation ratio could serve

5   as a performance metric for high energy materials.

6   **Keywords**: Femtosecond LIBS, Nitroimidazoles, Molecular CN and C_2 Emissions, Temporal

7   Dynamics, Intensity Ratios, Oxygen Balance

8   Corresponding author Tel.: +91 40 23138811/66798811; fax: +91 4023012800.

9   * e-mail: **svrsp@uohyd.ernet.in,soma_venu@uohyd.ac.in; # mathip@barc.gov.in**

10

1   # 1. Introduction

2   Over the last decade, there has been remarkable interest in exploring laser based

3   techniques[1-5], such as laser induced breakdown spectroscopy (LIBS), Raman, terahertz,

4   photoacoustic techniques etc. for the detection of hazardous materials including explosives.

5   The major aim here is to achieve unambiguous detection of trace explosive molecules with

6   the ultimate goal of standoff detection capability for trace molecules. LIBS technique, which

7   has been successfully employed for elemental analysis of a wide range of materials,[6,7] is one

8   of the potential techniques for detection of explosives due to its standoff detection capability

9   along with its ability to detect ppm (parts per million) concentrations in real time. In recent

10   studies, LIBS in combination with several chemometric approaches has been employed for

11   detection/discrimination/identification of explosive molecules, land mines, chemical and

12   biological warfare agent stimulants on various surfaces including polymers, metals etc.[8-15.]

13   Moreover, the standoff detection capability and man-portable LIBS systems has also been

14   demonstrated by several research groups.[16-18] A single-shot standoff LIBS for the detection of

15   energetic materials at distances up to 45 m has also been efficaciously demonstrated.[13] In

16   other fields such as lithography, micromachining, and medical applications the pre-eminence

17   of fs pulses usage over ns pulses has been indisputably established.[19] However, there are

18   certain issues that need to be addressed for application of LIBS for detection and

19   discrimination of explosive materials with high success rate for on-field applications.

20   Traditionally LIBS experiments have been performed with nanosecond (ns) pulses. Several

21   modifications such as double pulse LIBS and LIBS studies employing femtosecond (fs)

22   pulses have been shown to provide certain advantages for determination of various classes of

23   materials including explosives.[20-28] The characteristics of the laser induced plasma (LIP) are

24   found to depend strongly on the laser parameters such as pulse width, pulse energy, pulse

25   repetition rate, laser irradiance as well as the surrounding atmosphere. Femtosecond pulses

1 offer several advantages in LIBS applications such as (a) low fluence threshold, (b) precise

2 interrogation with the material, (c) efficient ablation, (d) lower continuum emission (e)

3 competency of traveling few kilometres of distance through filamentation process.[29] In fact

4 there are a few studies reported on filament induced LIBS wherein they demonstrate that the

5 pulses need not be focused to obtain the LIB spectra. Furthermore, a small amount of ablated

6 mass (as in the case of fs-LIBS) is an advantage when analyzing unique samples.The

7 relatively lower plasma temperature in the fs-LIBS also favours the formation of molecular

8 species such as CN and C_2 in explosives and related materials. Our earlier LIBS studies on a

9 series of energetic molecules clearly suggested the difference in molecular signatures in LIBS

10 data obtained with fs pulses.[30-32] Moreover, matrix effects are found to be detrimental in

11 determining traces of explosive molecules on different substrates (e.g. paper, metal, polymer,

12 leather etc.).[33-34] A deeper understanding of the interaction of fs pulses with material surface,

13 atmospheric contribution, focusing conditions etc. is, therefore, essential to further the

14 application of fs-LIBS technique.[35]

15 The most prevalent peaks in the LIB spectra of organic explosive related compounds

16 (ERCs) are from the elemental constituents, such as C, H, O, N and molecular emissions

17 from CN and C_2 species. Weaker emissions corresponding to CH, NH, OH species have also

18 been reported.[36] Many of the intermediates generated during the ablation process are not

19 detected by optical emission either due to their short lifetimes or due to emissions beyond the

20 detection range of the spectrometer. It is extremely difficult to ascertain the origin of

21 molecular emissions *i.e.* whether the species are released directly from native bonds by way

22 of fragmentation or are generated as a result of recombination with ambient constituents. The

23 plasma produced by fs-LIB is assumed to be in a state of local thermodynamic equilibrium

24 and is characterized by an excitation temperature (typically ~9000 K) and electron number

25 density (~1.5×10^{16} cm^{-3}) sufficiently high for sustaining the collisional processes. This gives

1   rise to a significant population of molecules in dissociative states which in turn opens up

2   many fragmentation/dissociative pathways.[37] As the plasma expands these species, created in

3   the breakdown zone, recombine with the surrounding atmospheric constituents to yield new

4   species. Despite plethora of reactions taking place in the organic plasma, the emission

5   spectra of the ERCs recorded in a narrow detection window (~ 800 ns) are seemingly alike.

6   Extensive time-resolved studies on expansion dynamics of graphite plume[38]

7   demonstrated the temporal evolution of fast and slow components of C_2 emission. The slow

8   component was assigned to dissociative processes (with long duration C_2 Swan emission)

9   whereas the fast component arose from recombination processes (within a narrow temporal

10   window). Recently, laser ablation molecular isotopic spectroscopic (LAMIS) studies[39] have

11   also indicated that generation of CN either involves atomic carbon or a species with single

12   carbon atom. The data obtained from a homologous series of nitro toluenes, mono-, di- and

13   tri-nitro toluene suggested that C_2 originated from unsubstituted carbon atoms in the ring.[40] A

14   recent study with 4-nitro aniline and 4-nitro toluene has also established a correlation

15   between the stoichiometry of the compound and the corresponding emission intensities.[41]

16   Several groups have presented various kinetic models to describe the formation of molecular

17   emission and have monitored the relative intensities of the atomic C/H/N/O emissions lines

18   towards discrimination of different molecules.[42-44] Hermann et al.[45] have modelled the local

19   thermal equilibrium plasma for the analysis of gas-phase reactions. Vivien at al.[46] employed

20   time- and space-resolved optical emission spectroscopic technique to investigate the kinetics

21   of excited plasma species C_2, CN and N_2^+ generated by an excimer laser ablation of graphite

22   sample in a low-pressure N_2 atmosphere. These studies have led to a better understanding of

23   the gas-phase reactions during the thin film deposition.

1　　　　Despite numerous studies and the availability of huge data on discrimination and

2　identification of ERCs, there is no clear understanding of the influence of molecular structure

3　(for e.g., the nature, position and number of substituent groups) on the optical emission

4　spectra. An exhaustive understanding of the fs (and ns) LIBS data correlating with the

5　molecular structure and surrounding environment is indispensable keeping in view the

6　impending applications of LIBS for detection of explosives. The knowledge of atmospheric

7　contribution to the LIBS data is indispensable for on-field/practical applications. In this work

8　we present the results from LIBS studies of seven different molecules belonging to a family

9　of ERCs (Nitroimidazoles), carried out in different environmental conditions (air, argon) and

10　pulse durations (fs and ns pulses). Nitroimidazoles have been used in medicines as antibiotic

11　drugs, radio sensitizers and recently explosives.[47] Imidazole derivatives with more than two

12　nitro groups, particularly 2, 4-dinitro imidazole (2,4-DNIm) are potential candidates for civil

13　and military applications due to its good thermal stability, impact and shock insensitivity,

14　better performance, economic and environmentally friendly synthesis. The nitroimidazoles

15　presented in this study were synthesized and characterized in our laboratory. The LIB spectra

16　were analysed for understanding (a) the influence of molecular structure i.e. type of bonds

17　(C-C, C=C, C-N and C=N) on the atomic and molecular emissions, (b) effect of surrounding

18　atmosphere on the fs and ns LIB spectra, (c) correlation between stoichiometric and intensity

19　ratios of molecular and atomic species, (d) effect of the number of substituents and their

20　position in the ring on the fragmentation pathways and (e) correlation between oxygen

21　balance and LIB spectra. Furthermore, time resolved spectroscopic studies of the plasma

22　induced by fs and ns laser pulses have been carried out to understand the temporal evolution

23　and possible reaction mechanisms of various molecular species. We have attempted to

24　correlate the spectral emission data with the chemical structure for this series of energetic

25　materials.

2. Experimental Set up

The fs LIBS data was recorded with two different 1 kHz fs laser systems located in two different labs (ACRHEM, University of Hyderabad, Hyderabad[31,48] and BARC, Mumbai). In general, the fs laser system comprises of a Ti-sapphire oscillator, a chirped pulse regenerative amplifier and a grating compressor. In both the LIBS experiments, the laser pulses with duration of ~50 fs, delivering ~1 mJ energy at a central wavelength 800 nm were used. The pulse-to-pulse energy fluctuation of the input laser pulses was <5%. Plasma for LIBS analysis was generated by focussing the 1 mJ pulse energy onto the surface of the sample pellets using a plano-convex lens of focal length 100 mm. The estimated beam diameter at focus was 12 ± 3 µm. The samples were mounted on a motorized Y-Z translational stage which is interfaced to LabVIEW and provided automated sample translation during data acquisition. This ensures a fresh area of the sample was always investigated. Collection of plasma emission in both the experimental setups was performed with a collimator fibre coupled to an Echelle grating spectrograph (Andor Mechelle ME5000) and detected by a thermoelectric cooled ICCD (Andor DH734-18mm-CCI-01U). The ICCD provided a spectral coverage from 200–900 nm with 0.1 nm wavelength resolution. The ICCD was gated in synchronization with the fs laser pulses to achieve good signal to noise ratio (S/N). The gate delay, gate width and the detection system were computer controlled through a digital delay generator embedded in the ICCD. The experiments aimed at understanding the influence of atmosphere (air versus Argon) were carried out at ACRHEM. Argon gas flow was directed through a nozzle onto the sample surface at the point of laser impact.

The ns LIBS data were recorded at ACRHEM and the details of the experimental setup are discussed in our previous works.[49,50] A Q-switched pulsed Nd-YAG laser system (SpitLight 1200, InnoLas) delivering ns pulses of wavelength at 532 nm with a pulse duration of ~7 ns and a repetition rate at 10 Hz was used. Typical pulse energy used in our

1 experiments was ~25 mJ. The ns laser pulses were focused on the target sample with a plano-

2 convex quartz lens with a focal length 100 mm. The fs-LIB spectra of all Nitroimidazoles

3 were recorded in air and argon atmospheres using a gate delay of 100 ns and a gate width of

4 800 ns. The ns-LIB spectra were recorded in air and argon atmospheres with a gate delay of

5 1100 ns and a gate width of 10 μs. For time resolved fs-LIBS studies, a gate width of 50 ns,

6 a step size of 50 ns was employed following an initial gate delay of 90 ns up to 590 ns. In ns

7 case, a series of time resolved spectra were recorded with a gate delay of 500 ns, gate width

8 of 500 ns, and a step size of 500 ns up to 5000 ns in both air and argon atmospheres.

9 **3. Sample preparation**

10 Seven novel ERCs are being studied for comparison of fs and ns spectral signatures in

11 air and argon atmospheres. These ERCs are a) Imidazole, Im ($C_3H_4N_2$) b) 4-Nitroimidazole,

12 4-NIm ($C_3H_3N_3O_2$) c) 1,4-Dinitroimidazole, 1,4-DNIm ($C_3H_2N_4O_4$) d) 2,4-Dinitroimidazole,

13 2,4-DNIm ($C_3H_2N_4O_4$) e) 1-Methyl-4-Nitroimidazole, 1M-4NIm ($C_4H_5N_3O_2$), f) 2-Methyl-

14 4(5)-Nitroimidazole, 2M-4(5)-NIm ($C_4H_5N_3O_2$), and g) 1-Methyl-2,4-Dinitroimidazole, 1M-

15 2,4-DNIm ($C_4H_4N_4O_4$). All the samples were prepared as pellets using manual hydraulic

16 press (4-6 metric tonnes of pressure and 3-4 minutes duration) with diameter of ~12 mm and

17 weight ranging from 600 to 800 mg with a thickness of 2-3 mm.

18 **4. Results and Discussions**

19 **4.1 fs and ns-LIB spectral signatures in air and argon atmospheres**

20

21 The fs-LIB spectra of Imidazole recorded in air is shown in Fig.1a. The LIB emission

22 spectra evidently are dominated by molecular emission bands corresponding to CN and C_2.

23 The CN molecular bands corresponding to Δυ values of −1, 0 and +1, were observed at 357–

24 360 nm, 384–389 nm and 414–423 nm respectively. Amongst these, the molecular emission

1   at 388.32 nm corresponding to CN violet band ($B^2\Sigma^+ \rightarrow X^2\Sigma^+$) ($\Delta v = 0$ sequence) was the

2   strongest. C_2 molecular bands corresponding to $\Delta v = -1, 0$ and $+1$ transitions were located

3   in the spectral regions of 460–475 nm, 510–520 nm and 550–565 nm respectively. The

4   strongest C_2 emission was observed for Swan band ($D^3\Pi^g \rightarrow a^3\Pi^u$) at 516.52 nm

5   ($\Delta v=0$ sequence). The atomic emissions corresponding to the elemental constituents C(I)

6   (247.86 nm), H_α (656.33 nm), O(I) (777.42 nm), N(I) triplet lines (742.46 nm, 744.28 nm,

7   746.85 nm), N (868.23 nm) are relatively weaker. The ns-LIB spectra (Fig. 1a) demonstrated

8   additional features such as unresolved O(I) triplet lines (777.23 nm, 777.42 nm and 777.51

9   nm), N(I) emission lines at 818.49 nm, 818.79 nm, 821.04 nm, 821.69 nm, 824.50 nm and

10   863.18 nm along with weaker atomic emissions of Ca(I), Na(I) and Fe(I), which possibly

11   were from the sample impurities assimilated during the pellet preparation. The overall signal

12   levels in fs spectra were superior to the ns spectra. Fig. 1b shows the fs and ns-LIB spectra of

13   imidazole recorded in argon atmosphere. In addition to the spectral features discussed above,

14   Ar(I) atomic emissions lines were observed at 696.61 nm and in the spectral region of 750

15   nm to 850 nm. The details of the peaks observed in fs and ns LIB spectra of seven

16   nitroimidazoles recorded in air and argon atmospheres are summarized in Table 1. Strong CN

17   molecular emissions corresponding to different vibrational transitions ($\Delta v = -1, 0$ and $+1$) are

18   observed for all these compounds whereas C_2 molecular bands have been observed only for

19   Im, 4-NIm,1M-4NIm and 2M-4(5)-NIm. The dinitroimidazoles (1,4-DNIm,2,4-DNIm and

20   1M-2,4-DNIm) spectra exhibited very weak C_2 emissions [see supporting information (SI)

21   Fig. 1, Fig. 2 and Fig. 3]. The corresponding bar graph (data presented in Fig.2) shows

22   variation in intensity distribution thus indicating the feasibility of qualitatively distinguishing

23   different compounds. Hence, it is of interest to study any correlation that exists between the

24   emission intensities and chemical structure of these molecules (SI Fig. 4).

1 **4.2 Correlation between atom percent (C, H, N and O), stoichiometric ratios and**

2 **corresponding atomic emission intensities (ratios)**

3 We have attempted to study the degree of correlation between the atomic spectral lines of

4 carbon (247.86 nm), H_α (656.32 nm), Oxygen (777.42 nm) and Nitrogen (868.68 nm) and

5 also the molecular emissions of CN (388.32 nm) and C_2 (516.52 nm) using fs LIBS data

6 recorded in air and argon atmospheres. Table 2 shows the percentages of elemental

7 constituents (C, H, N and O), bonds (C-C, C=C, C-N and C=N) and oxygen balance (OB)

8 values, and for all the Imidazoles studied (SI Table 1). The percentage of atomic elements (C,

9 H, N and O) and bond type (C-C, C=C, C-N and C=N) were calculated from the molecular

10 formula ($C_aH_bN_cO_d$) of the compound using the equations:

11
$$\% \ element \ = \frac{Number \ of \ elemental \ atoms \ present \ in \ the \ molecule}{Total \ number \ of \ atoms \ present \ in \ the \ molecule} \times 100 \quad (1a)$$

12
$$\% \ bond \ = \frac{Number \ of \ particlar \ bond \ present \ in \ the \ molecule}{Total \ number \ of \ bonds \ present \ in \ the \ moleucule} \times 100 \quad (1b)$$

13 When the % for every element in the compound is added together, the result will be 100.

14 Percentages of all atomic elements and bond types were measured with this simple method

15 for all the Nitroimidazoles studied. The correlation was performed by estimating the linear

16 regression coefficient (r^2) values. Figures 3a-g depict the correlation data between

17 stoichiometric values (i.e. % O, H, N and C) and the atomic emission intensities for each

18 sample with fs excitation in argon and air atmospheres. The correlation of O emission

19 intensity in air with %O atom [Fig. 3(a)] was poor ($r^2 = 0.62$) and it did not show any

20 improvement in argon atmosphere [($r^2 = 0.60$, Fig. 3(b)]. However, by using normalized

21 intensity as suggested by Lucia *et al.*[14], we observed a significant improvement in the

22 correlation ($r^2 = 0.86$, Fig. 3c). The atomic emission lines of interest are normalised with

23 another atomic emission line of an internal standard (in this case argon) in order to minimize

1   the differences in laser-materials interactions. Ideally, the atomic lines so chosen should have

2   similar upper energy levels and closely located emission wavelengths for best normalization.

3   It may be pointed out here that the upper energy levels for the O(I) (777.42 nm) and Ar(I)

4   (772.42 nm) emission lines are not similar [86627 cm^{-1} for O(I) as compared to 107496 cm^{-1}

5   for Ar(I)]. The H(I) emission intensity in ambient atmosphere correlated well with %H atom

6   (r^2=0.85) for ablation in air but deteriorated in argon atmosphere (r^2=0.72) (Figures 3d,e).

7   The C(I) emission intensity exhibited poor correlation with %C atom in air (r^2=0.51) with

8   marginal improvement in argon (r^2=0.68) (Figures 3 f,g). It needs to be mentioned here that

9   since there were no Ar(I) emission satisfying the selection criteria discussed above,

10   normalization procedures could not be carried out for C(I) and H lines. Furthermore, we have

11   studied the correlation between stoichiometric elemental ratios and emission intensity ratios

12   for each sample. Figures 4(a-f) illustrate the extent of correlation between O/C, O/H and N/H

13   emission intensity ratio and the corresponding stoichiometric ratios in air and argon

14   atmospheres. The relatively superior correlation coefficients observed for all ratios in argon

15   atmosphere indicates that the LIBS spectral lines faithfully reflected the changing elemental

16   ratios. Generally r^2 value >0.9 for a particular ratio represents a strong correlation.

17   **4.3 Correlation between molecular emission intensities and molecular structure**

18   All the compounds in the imidazole series (Im, 4-NIm, 2,4-DNIm, 1M-4NIm and 1M-

19   2,4-DNIm) exhibited a weak NH ($A^3\pi_i$-$X^3\Sigma^-$) system of (0,0) vibrational transition emission

20   band near 336 nm. Serrano *et al.*[51] proposed, for the first time, the formation pathways of CH,

21   NH, and OH radicals in fs laser-produced plasma of molecular solids. Their data clearly

22   suggests the direct release of native molecular bonds as a substantial source that populates fs

23   laser-produced plasma with NH radicals. In the present case the first three compounds have

24   native N-H bonds whereas the methyl substituted 4-NIm and 2,4-DNIm are devoid of any

1 native NH bonds. Further, the absence of any correlation between NH intensity and %N or

2 %H suggests that NH may also be formed by recombination processes taking place in the

3 plasma (SI Fig. 5). In the following discussion, we try to probe whether the molecular

4 structure of these compounds has any bearings on emission intensities of C_2 (Swan) and CN

5 (Violet) molecular bands in the LIB spectrum.

6 **4.3.1 CN emission**

7 The strongest CN emission line at 388.32 nm is considered in this section. All the

8 compounds in the Imidazole series have native C-N and C=N bonds, so CN emission may

9 come from the direct emission of native CN bonds. But it is evident from Figures 5a-b, the

10 CN emission intensities do not seem to correlate well with the %C=N in air and the

11 summation of %C-N and %C=N bonds in argon for these compounds. This suggests that in

12 addition to CN emission from native CN bonds, there may be secondary sources for CN

13 generation such as the reaction between C_2 (formed via native C=C bonds or C_2 formed by

14 recombination in the plasma) and atmospheric N_2, as well as the recombination of C with N

15 or N_2. In our LIB emission spectrum we did not observe any signature of NO owing to its

16 short life time and, probably, because of interference from the CN band (421.6 nm).[52] It may

17 be mentioned here that Delgado *et al.*[53] had detected NO and CH_n by laser ablation mass

18 spectroscopic methods.

19 **4.3.2 C_2 emission**

20 Among the seven compounds studied in the imidazole series, only Im, 4-NIm, 1M-4NIm

21 and 2M-4(5)-NIm exhibited strong signatures of C_2. On the other hand, weak signatures of C_2

22 emission were observed in 1,4-DNIm, 2,4-DNIm and 1M-2,4-DNIm. Although, Figures 5c-d

23 clearly demonstrate a superior correlation between the percentage (%) of carbon atoms and

24 the strongest C_2 peak intensities in air and argon atmospheres, we failed to observe any

1   correlation between the C_2 intensities and %C=C bonds in both the atmospheres (Figure 5e-

2   f). This behaviour is indicative of the occurrence of two routes for the formation of C_2 species

3   as suggested by Harilal *et al.*.[54] They observed that in the low intensity regime, C_2 species

4   were formed by the direct fragmentation of the parent molecule and dissociation of large

5   carbon clusters with the final release of C_2 dimers. In the high intensity regime,

6   recombination processes played a predominant role in the formation of C_2. In two separate

7   works, St-Onge *et al.*[55] and Portnov *et al.*[56] had suggested the presence of C=C and C≡C

8   bonds as a prerequisite for the observance of C_2 emission. The C_2 species could be formed

9   either by fragmentation of the aromatic ring or from reactions between the resulting

10 hydrocarbon species present in the plasma. This was further corroborated by Lucena *et al.*[40]

11 who had observed significant C_2 emission in a series of aromatic compounds but extremely

12 weak or zero C_2 intensity in the case of RDX and PETN both of which are devoid of C=C

13 bonds. These studies have indicated that the ring opening and fragmentation processes are

14 significantly affected by changes in the stability of the ring. Further, they experimentally

15 verified this conjecture by ablating a series of substituted nitrotoluenes. The C_2 emission

16 intensity decreased substantially with the increase in number of nitro groups. They have

17 reported that C_2 emission might be due to fragments from unsubstituted C atoms formed after

18 ring opening. At this point we are tempted to understand the influence of type and number of

19 substituents on C_2, CN intensities and fragmentation pathways in the Imidazole series.

20   Let us consider the series Im, 4-NIm, 2,4-DNIm, 1M-4NIm and 1M-2,4-DNIm. The

21 C_2 emission intensity decreases along this series (Fig. 6). The significantly high C_2 yield in

22 Imidazole can be attributed to the presence of one unsubstituted C=C bond (this is zero for 4-

23 NIm and 2,4-DNIm); the fragments formed from unsubstituted carbon atoms following ring

24 opening give rise to a high C_2 yield. 4-NIm and 2,4-DNIm do not possess any unsubstituted

25 C=C bonds, yet C_2 emission band intensity in 4-NIm is substantially higher than 2,4-DNIm.

1 This trend can be attributed to difference in the number of nitro-functional groups along this

2 series. The nitro group by way of inductive effect pulls the electrons towards it and

3 introduces significant charge separation on the carbon atom to which it is attached.

4 Additionally the highly electronegative atom pulls the electron pair of the multiple bond

5 which results in withdrawal of electron density from the aromatic ring, thus giving rise to

6 different canonical forms. Thus, resonance causes decrease of electron density in the

7 Imidazole ring. Both the resonance and inductive effect act in a synergistic fashion. The drain

8 of electrons from the ring makes it easily susceptible to atomization. This is reflected by the

9 low C_2 intensity and large CN emission signal in 4NIm. An increase in the number of

10 electron withdrawing nitro groups, as in 2-4-DNIm, further weakens the ring structure

11 making it more prone to atomization *i.e.* a large CN signal and almost zero C_2 emission. This

12 argument is in line with results from quantum chemical studies by Su *et al*.[57] They found that

13 the increase in the number of NO_2 groups on the Imidazole ring reduces the stability of the

14 molecule, which is characterized by the decrease of the weakest $C-NO_2$ bond energy in Table

15 4. Bond dissociation energies (BDEs) provide valuable information in understanding the

16 stability of nitroimidazoles. The stability of a compound depends on temperature, nature of

17 materials, and substituent groups. The weak C_2 emission band in 2,4-DNIm also suggests that

18 C_2 formation does not proceed via the recombination pathway.

19 Another interesting observation is the strong correlation between C_2 emission

20 intensity and the Oxygen atom % in both air and argon atmospheres [Figures 7a,b]. The C_2

21 emission intensities decreased with increasing oxygen content. This suggests possible

22 scavenging of C and C_2 species by oxygen which may proceed by the following

23 mechanism:[58]

$$C + O \rightarrow CO \qquad (2)$$

$$C_2 + O \rightarrow CO + C \qquad (3)$$

$$C_2 + O_2 \rightarrow 2CO \qquad (4)$$

1   Further, the effect of alkyl substitution with regard to atomization/fragmentation of

2   the ring structure in nitro imidazoles can be understood by comparing the C_2 emission

3   intensities in 1M-4NIm Vs 4-NIm and 1M-2,4-DNIm Vs 2,4-DNIm). The CH_3 group gives

4   rise to a special resonance called hyper conjugation or no-bond resonance which involves the

5   interaction of sigma electrons. This relatively weaker intra molecular charge transfer (in

6   comparison to strong electron releasing groups like $-NH_2$ and $-OH$) does not extend

7   πelectron delocalization. Although the NO_2 group is electron withdrawing, the CH_3 group

8   does not allow resonance, which leads to partial localization of single and double bonds.

9   Consequently 1M-4NIm resists atomization thereby exhibiting nearly similar C_2 intensities as

10   4-NIm. Similar argument holds good for 1M-2,4-DNIm versus 2-4-DNIm (SI Fig. 6).

11   Further evidence of the competition between fragmentation and atomization can be

12   seen in the LIP emission spectra of six membered aromatics like 4-nitro aniline and 4-nitro

13   phenol. The OH group is more electron releasing than $-NH_2$; the charge transfer from the

14   donating group through the πsystem to the accepting group gives rise to a large number of

15   resonant structures. The relatively larger aromatic π- electron delocalization in 4NP as

16   compared to 4NA is manifested as a higher CN/C_2 ratio (SI Table 2).The nature of the

17   substituents thus plays a crucial role in favouring/restricting π electron delocalization which

18   in turn dictates the fragmentation/atomization as well as the (C_2/CN) relative intensities.

19   **5. Decoding the LIBS spectra in terms of performance of energetic material**

20   **correlating with oxygen balance**

21

22   The detonation properties of energetic materials depend on their oxygen balance

23   which is a measure of the degree to which an explosive can be oxidized. It is calculated from

1   the empirical formula of the compound and is defined as the ratio of the oxygen content of a

2   compound to the total oxygen required for the complete oxidation of all carbon, hydrogen

3   and other oxidizable elements to CO_2, H_2O, etc. Lothrop and Handrick[59] provided the

4   procedure for calculating the oxygen balance of a nitro compound with molecular formula

5   $C_aH_bN_cO_d$. The oxygen balance (Ω) for a nitro compound with molecular formula $C_aH_bN_cO_d$

6   as defined by Lothrop and Handrick[59], is expressed as:

7   $$\Omega = (d-2a-b/2)\ 1600/M \qquad (5)$$

8   where M is the relative molecular mass of the energetic material

9   The molecule is said to have zero oxygen balance if it contains just enough oxygen to

10 convert all the carbon to carbon dioxide, hydrogen to water, and all of its metal to metal

11 oxide; in this case the heat of explosion will be maximum. The oxygen balance will be

12 positive if it contains more oxygen than is needed and a negative if it contains less oxygen

13 than is required. Energetic materials are classified as either oxygen deficient or oxygen rich.

14 Most energetic materials are oxygen deficient. The oxygen balance calculated for the

15 Imidazole series of compounds studied here is listed in Table 2. In our recent work on

16 nitropyrazoles, we reported a correlation between LIBS data of Nitropyrazoles in argon

17 atmosphere with oxygen balance (OB).[32] In the present study, the correlation between the

18 LIB signal intensity of atomic and molecular species with oxygen balance has been explored

19 for fs excitations in imidazole series of compounds in argon and air atmospheres.

20 Figures 8(a) and 8(b) depict the variation in the signal intensity of CN (388.32 nm),

21 C_2 (516.52 nm) and C (247.86 nm) emissions with OB using fs excitations in air and argon

22 atmosphere respectively. The CN Violet band, C_2 Swan band and C atomic emission

23 intensities decreased with increasing OB. As the number of nitro groups increases along the

24 series of Im, 4-NIm, 2,4-DNIm, the oxygen balance tends to -30. The concomitant rise in

1　atomisation /fragmentation and CN/C_2 ratio in both air and argon atmospheres is clearly seen

2　in the plot of CN/C_2 versus OB (Figures 8 c,d). As the OB tends to zero, atomization

3　becomes the dominant pathway in the laser produced plasma. Therefore, the

4　atomisation/fragmentation ratios could serve as a performance metric for high energy

5　materials (SI Fig. 7). The CN/C_2 ratio was lower in argon atmosphere than air with ns

6　excitation due the C_2 formed the partial fragmentation of the parent molecule and there is no

7　nitrogen influence on the molecule from the atmospheres (SI Fig. 8). Serrano et al.[8]

8　presented a diagnostic tool for inferring the predominance of atomization or fragmentation

9　reactions in the plasma, which was the ratio of CN/C_2.

10 6. Temporal studies of molecular emissions (CN, C$_2$) and C atomic line in

11 air and argon atmospheres with fs and ns pulses

12　　　To gain a deeper insight into possible reaction mechanisms for CN and C_2 formation,

13　time-resolved LIBS (TRELIBS) studies were carried out using both fs and ns laser pulses.

14　TRELIBS spectra have been recorded for Im, 1,4-DNIm and 2M-4(5)-NIm with fs excitation

15　and Im, 4-NIm, 1,4-DNIm and 1M-4NIm with ns excitation. The molecular bands CN (Δv=0)

16　at 388.32 nm, C_2(Δv=0) at 516.52 nm and atomic emission carbon remain clearly observed

17　up to 590 ns from the starting gate delay with fs excitation. The atomic emission line H of

18　hydrogen remained significant up to 390 ns. In the case of ns excitation the molecular bands

19　of CN (Δv=0) at 388.32 nm and C_2 (Δv=0) bands at 516.52 nm, atomic emissions C, H were

20　observed for longer delays. In the ns excitation case (argon) the intensity of the continuum

21　reduced significantly at about 1500 ns (see data presented in SI Fig. 9). Figure 9 presents the

22　temporal evolution data of molecular bands CN (388.32 nm), C_2 (516.52 nm) and C (247.86

23　nm) with fs and ns excitation in argon atmosphere. The time resolved decays of molecular

24　bands CN, C_2 and atomic emission C were fitted using single exponential function. The

1 decay constants were calculated for CN, C_2 bands and C line using exponential decay fits to

2 the experimental using the equation

3
$$y = A_1 \times \exp(-x/t_1) + y_0 \qquad (6)$$

4 The fitted decay rates for CN, C_2 and C are summarized in Table 3 (and also in SI Table 3

5 and SI Figures 10, 11 and 12).

6   Aguilera et al.[60] had shown that argon is efficiently heated by inverse Bremsstrahlung,

7 and, therefore, the plasma created in argon have higher electron temperatures and electron

8 densities thus justifying the higher emission intensities observed. It needs to be pointed out

9 here that the decay times obtained for these species in air and argon atmosphere using ns

10 excitation do not exhibit a clear trend. The multiple generation pathways arising out of

11 atmospheric interference hinders the interpretation of time resolved data recorded in air. The

12 data recorded in argon atmosphere is devoid of such interferences and can be used to gain

13 insight into the reaction mechanisms. The persistence (decay times) for CN emission from fs

14 excitation is relatively larger in argon atmosphere. The higher plasma temperature and

15 electron density may aid the generation of CN by recombination processes. The longest decay

16 times for C_2 species in argon atmosphere were observed for Imidazole (431 ns) which is

17 devoid of oxygen. The decay times for other compounds considered here decreased with

18 increasing oxygen content. This observation seems to be consistent with the mechanism cited

19 in equations 2-4. Further investigations are warranted to confirm this. A very recent review

20 article by Labutin et al.[61] vindicates the usage and unique possibilities of fs pulses for LIBS

21 studies. This article clearly outlines the various advantages of fs pulses for LIBS studies and

22 we hope that these can be extended to studies of explosive molecules thereby enabling

23 technologies for stand-off detection.

24

1 ## 7. Conclusions

2 We have used fs and ns pulses to record the LIB spectra of seven energetic molecules

3 (nitroimidazoles) in air and argon atmospheres. We have investigated the behaviour of

4 molecular (CN, C_2 and NH) and atomic (C, H, N and O) emissions in air and argon

5 atmospheres. The comparison of fs and ns LIB spectra in air and argon established the

6 signature of the sample constituents in the plasma region. We observed a strong signature

7 corresponding to molecular species in fs excitation and atomic species in ns excitation. CN

8 emission was dominant for ablations carried out in air, whereas in C_2 emission features were

9 prominent in the LIB spectra recorded in argon atmosphere. Usage of normalised intensities

10 led to a significant improvement in the correlation between atomic emission intensities and

11 the corresponding stoichiometric values. A good correlation coefficient seen for all ratios in

12 argon atmosphere indicates that the LIBS spectral lines faithfully reflect the changing

13 elemental ratios. Time resolved data have given valuable insight into possible reaction

14 mechanisms of various molecular species. The molecular emission intensities in the LIP

15 spectra of these compounds exhibited a strong dependence on the number and position of

16 substituents, particularly the nitro group. Both the resonance and inductive effect due the

17 nitro group drain out the electrons from the ring thereby making it easily susceptible to

18 atomization. This led to a reduction in C_2 intensity and increment in CN intensity with

19 increase in the number of electron withdrawing nitro groups. Further, we observed a strong

20 correlation between C_2 emission intensity and the % of oxygen atoms in the molecule; the C_2

21 emission intensity decreased with increase in oxygen content. Our detailed studies and

22 analyses clearly suggest that atomization/fragmentation ratio could serve as a performance

23 metric for discriminating high energy materials.

24

1 ## 8. Acknowledgements

7

9. References

1 D. A. Cremers and L. J. Radziemski, *Handbook of Laser-Induced Breakdown Spectroscopy*, Wiley, 2006.

2 A.W. Fountain III, S.D. Christesen, R.P. Moon, J.A. Guicheteau, E.D. Emmons, Recent advances and remaining challenges for the spectroscopic detection of explosive threats, *Appl. Spectrosc.*, 2014, **68(8)**, 795-811.

3 P. M. Pellegrino, E. L. Holthoff, M. E. Farrell, eds., *Laser-Based Optical Detection of Explosives*, 2015, CRC Press.

4 J. B. Johnson, S. D. Allen, J. Merten, L. Johnson, D. Pinkham, and S. W. Reeve, Standoff methods for the detection of threat agents: A review of several promising laser-based techniques, *J. Spectros.*, 2014, **2014**, Article ID 613435.

5 M. R. Leahy-Hoppa, J. Miragliotta, R. Osiander, J. Burnett, Y. Dikmelik, C. McEnnis, J. B. Spicer, Ultrafast laser-based spectroscopy and sensing: Applications in LIBS, CARS, and THz spectroscopy, *Sensors,* 2010, **10,** 4342-4372.

6 D.W. Hahn, N. Omenetto. Laser-induced breakdown spectroscopy (LIBS), part I: review of basic diagnostics and plasma-particle interactions: still-challenging issues within the analytical plasma community, *Appl. Spectrosc.,* 2010, **64**, 335–66.

7 D.W. Hahn, N. Omenetto, Laser-induced breakdown spectroscopy (LIBS), part II: review of instrumental and methodological approaches to material analysis and applications to different fields, *Appl. Spectrosc.,* 2010, **66**, 347–419.

8 J. Serrano, J. Moros, and J.J. Laserna, Sensing signatures mediated by chemical structure of molecular solids in laser-induced plasmas, *Anal. Chem.,* 2015, **87**, 2794−2801.

9   R. S. Harmon, F. C. De Lucia Jr., A. La Pointe, R. J. Winkel Jr. and A.W. Miziolek, LIBS for landmine detection and discrimination, *Anal. Bioanal. Chem.*, 2006, **385**, 1140-1148.

10   L. Mercadier, J. Hermann, C. Grisolia, A. Semerok, Diagnostics of nonuniform plasmas for elemental analysis via laser-induced breakdown spectroscopy: demonstration on carbon-based materials, *J. Anal. At. Spectrom.,* 2013, **28(9)**, 1446-1455.

11   M. Abdelhamid, F. J. Fortes, M. A. Harith and J. J. Laserna, Analysis of explosive residues in human fingerprints using optical catapulting–laser-induced breakdown spectroscopy, *J. Anal. At. Spectrom.*, 2011, **26**, 1445-1450.

12   J.L. Gottfried, F.C. De Lucia Jr., C.A. Munson and A.W. Miziolek, Strategies for residue explosives detection using laser-induced breakdown spectroscopy, *J. Anal. At. Spectrom.*, 2008. **23**, 205-216.

13   C. Lopez-Moreno, S. Palanco, J. Javier Laserna, F. DeLucia Jr, A. W. Miziolek, J. Rose, R. A. Walters and A. I. Whitehouse, Test of a stand-off laser-induced breakdown spectroscopy sensor for the detection of explosive residues on solid surfaces, *J. Anal. At. Spectrom.*, 2006, **21**, 55-60.

14   F. C. De Lucia and J. L. Gottfried, Influence of Molecular Structure on the Laser-Induced Plasma Emission of the Explosive RDX and Organic Polymers, *J. Phys. Chem. A*, 2013, **117**, 9555-9563.

15   J. L. Gottfried, F. C. De Lucia Jr., C. A. Munson and A. W. Miziolek, Strategies for residue explosives detection using laser-induced breakdown spectroscopy, *J. Anal. At. Spectrom.*, 2008, **23**, 205-216.

1   16   F.C. De Lucia Jr., J.L. Gottfried, C. A. Munson, A.W. Miziolek, Multivariate analysis

2   of standoff laser-induced breakdown spectroscopy spectra for classification of

3   explosive-containing residues, *Appl. Opt.,* 2008, **47(31),** G112-G122.

4   17   R. Gonzalez, P. Lucena, L. M. Tobaria and J. J. Laserna, Standoff LIBS detection of

5   explosive residues behind a barrier, *J. Anal. At. Spectrom.*, 2009, **24**, 1123-1126.

6   18   I. Gaona, J. Moros, J. J. Laserna, New insights into the potential factors affecting the

7   emission spectra variability in standoff LIBS, *J. Anal. At. Spectrom.*, 2013, **28(11)**,

8   1750-1759.

9   19   B.N. Chichkov, C. Momma, S. Nolte, Femtosecond, picosecond and nanosecond laser

10   ablation of solids, *Appl. Phys. A,* 1996, **63,** 134–142.

11   20   S. S. Harilal, J. Freeman, P. Diwakar and A. Hassanein, Femtosecond laser ablation:

12   Fundamentals and applications, in *Laser-Induced Breakdown Spectroscopy*, ed.'s S.

13   Musazzi and U. Perini, Springer Berlin Heidelberg. 2014, vol. 182, ch. 6, pp. 143-

14   166.

15   21   J. R. Freeman, S. S. Harilal, P. K. Diwakar, B. Verhoff, A. Hassanein, Comparison of

16   optical emission from nanosecond and femtosecond laser produced plasma in

17   atmosphere and vacuum conditions, *Spectrochim. Acta, Part B,* 2013, **87,** 43-50.

18   22   M. Oujja, M. Sanz, F. Agua, J. F. Conde, M. Garc´ıa-Heras, A. D´avila, P. O˜nate, J.

19   Sanguino, J. R. V´azquez de Aldana, P. Moreno, M. A. Villegas and M. Castillejo,

20   Multianalytical characterization of Late Roman glasses including nanosecond and

21   femtosecond laser induced breakdown spectroscopy, *J. Anal. At. Spectrom.*, 2015, **30**,

22   1590-1599.

23   23   M. Baudelet, L. Guyon, J. Yu, J.-P. Wolf, T. Amodeo, E. Fréjafon and P. Laloi,

24   Femtosecond time-resolved laser-induced breakdown spectroscopy for detection and

identification of bacteria: A comparison to the nanosecond regime, *J. Appl. Phys,* 2006, **99**, 084701-9.

24 R. K. Gill, F. Knorr, Z.J. Smith, M. Kahraman, D. Madsen, D.S. Larsen, S. Wachsmann-Hogiu, Characterization of femtosecond laser-induced breakdown spectroscopy (fsLIBS) and applications for biological samples, *Appl. Spectrosc.,* 2014, **68**, 949-954.

25 G. Gustinelli, A. de Carvalho, J. Moros, D. Santos Jr., F. J. Kruga, J. J. Laserna, Direct determination of the nutrient profile in plant materials by femtosecond laser-induced breakdown spectroscopy, *Anal. Chim. Acta,* 2015, **876**, 26-38.

26 M. Kotzagianni, S. Couris, Femtosecond laser induced breakdown for combustion diagnostics, *Appl. Phys. Lett.,* 2012, **100,** 264104.

27 T. Ahmido, A. Ting and P. Misra, Femtosecond laser-induced breakdown spectroscopy of surface nitrate chemicals, *Appl. Opt.*, 2013, **52**, 3048-3057.

28 F. C. De Lucia, J. L. Gottfried and A. W. Miziolek, Evaluation of femtosecond laser-induced breakdown spectroscopy for explosive residue detection, *Opt. Express*, 2009, **17**, 419-425.

29 E. L. Gurevich, R. Hergenroeder, Femtosecond laser-induced breakdown spectroscopy: physics, applications, and perspectives, *Appl. Spectrosc.,* 2007, **61**, 233A–242A.

30 S. Sreedhar, E. Nageswara Rao, G. Manoj Kumar, S. P. Tewari and S. Venugopal Rao, Molecular formation dynamics of 5-nitro-2,4-dihydro-3H-1,2,4-triazol-3-one,1,3,5 trinitroperhydro-1,3,5-triazine, and 2,4,6-trinitrotoluene in air, nitrogen, and argon atmospheres studied using femtosecond laser induced breakdown spectroscopy, *Spectrochim. Acta, Part B*, 2013, **87**, 121-129.

31   S. Sunku, M. K. Gundawar, A. K. Myakalwar, P. P. Kiran, S. P. Tewari and S. Venugopal Rao, Femtosecond and nanosecond laser induced breakdown spectroscopic studies of NTO, HMX, and RDX, *Spectrochim. Acta, Part B*, **79–80**, 31-38.

32   E. Nageswara Rao, S. Sreedhar and S. Venugopal Rao, Femtosecond Laser-Induced Breakdown Spectroscopy Studies of Nitropyrazoles: Effect of Varying Nitro Groups, *Appl. Spectros.,* 2015, **69(11),** 1342-1354.

33   B. Zhang, M. He, W. Hang, and B. Huang, Minimizing matrix effect by femtosecond laser ablation and ionization in elemental determination, *Anal. Chem.,* 2013, **85,** 4507−4511.

34   H.L. Xu, G. Méjean, W. Liu, Y. Kamali, J.-F. Daigle, A. Azarm, P.T. Simard, P. Mathieu, G. Roy, J.-R. Simard, S.L. Chin, Remote detection of similar biological materials using femtosecond filament-induced breakdown spectroscopy, *Appl. Phys. B.,* 2007, **87,** 151-156.

35   C.A. Zuhlke, J. Bruce, T.P. Anderson, D.R. Alexander, and C.G. Parigger, A fundamental understanding of the dependence of the laser-induced breakdown spectroscopy (LIBS) signal strength on the complex focusing dynamics of femtosecond laser pulses on either side of the focus, *Appl. Spectrosc.,* 2014, **68,** 1021-1029.

36   T. Delgado, J. M. Vadillo and J. J. Laserna, Primary and recombined emitting species in laser induced plasmas of organic explosives in controlled atmospheres, *J. Anal. At. Spectrom.*, 2014, **29**, 1675-1685.

37   N. M Shaikh, B. Rashid, S. Hafeez, Y. Jamil and M. A. Baig, Measurement of electron density and temperature of a laser-induced zinc plasma, *J. Phys. D: Appl. Phys.,* 2006, **39(7)**, 1384-1391.

38   C. G. Parigger, J. O. Hornkohl, A. M. Keszler, and L. Nemes, Measurement and analysis of atomic and diatomic carbon spectra from laser ablation of graphite, *Appl. Opt.*2003, **42**, 6192-6198.

39   M. Dong, G. C. Y. Chan, X. Mao, J. J. Gonzalez, J. Lu and R. E. Russo, Elucidation of C and CN formation mechanisms in laser-induced plasmas through correlation analysis of carbon isotopic ratio, *Spectrochim. Acta, Part B*, 2014, **100**, 62-69.

40   P. Lucena, A. Doña, L. M. Tobaria and J. J. Laserna, New challenges and insights in the detection and spectral identification of organic explosives by laser induced breakdown spectroscopy, *Spectrochim. Acta, Part B*, 2011, **66**, 12-20.

41   S. Rai and A.K. Rai, Characterization of organic materials by LIBS for exploration of correlation between molecular and elemental LIBS signals, *AIP Advances*, 2011, **1**, 042103-11.

42   M. Dong, X. Mao, J. J. Gonzalez, J. Lu and R. E. Russo, Time-resolved LIBS of atomic and molecular carbon from coal in air, argon and helium, *J. Anal. At. Spectrom.*, 2012, **27**, 2066-2075.

43   V. I. Babushok, F. C. DeLucia Jr, P. J. Dagdigian, J. L. Gottfried, C. A. Munson, M. J. Nusca and A. W. Miziolek, Kinetic modeling study of the laser-induced plasma plume of cyclotrimethylenetrinitramine (RDX), *Spectrochim. Acta, Part B*, 2007, **62**, 1321-1328.

44   P. J. Dagdigian, A. Khachatrian and V. I. Babushok, Kinetic model of C/H/N/O emissions in laser-induced breakdown spectroscopy of organic compounds, *Appl. Opt.*, 2010, **49**, C58-C66.

45   J. Hermann and C. Dutouquet, Local thermal equilibrium plasma modeling for analyses of gas-phase reactions during reactive-laser ablation, *J. Appl. Phys.*, 2002, **91**, 10188-10193.

46   C. Vivien, J. Hermann, A. Perrone, C. Boulmer-Leborgne, A. Luches, A study of molecule formation during laser ablation of graphite in low-pressure nitrogen, *J. Phys. D: Appl. Phys.*, 1998, **31(10)**, 1263-1272.

47   L. Larina, and L. Lopyrev, Nitroazoles: Synthesis, Structure and Applications, Springer, New York, 2009.

48   N. R. Epuru, S. Sunku, M. K. Gundawar and Venugopal Rao Soma, Femtosecond Time Resolved Laser Induced Breakdown Spectroscopy Studies of Nitroimidazoles, *12th International Conference on Fiber Optics and Photonics,* OSA Technical Digest (online) (Optical Society of America, 2014), paper S5A.30.

49   S. Sreedhar, M. K. Gundawar and S. Venugopal Rao, Laser Induced Breakdown Spectroscopy for Classification of High Energy Materials using Elemental Intensity Ratios, *Def. Sci. J.,* 2014, **64***,* 332-338.

50   A. K. Myakalwar, S. Sreedhar, I. Barman, N. C. Dingari, S. Venugopal Rao, P. Prem Kiran, Surya. P. Tewari, G. Manoj Kumar, Laser-induced breakdown spectroscopy-based investigation and classification of pharmaceutical tablets using multivariate chemometric analysis, *Talanta,* 2011, **87**, 53-59.

51   J. Serrano, J. Moros, J.J. Laserna, Exploring the formation routes of diatomic hydrogenated radicals using femtosecond laser-induced breakdown spectroscopy of deuterated molecular solids, *J. Anal. At. Spectrom.*, 2015, **30**, 2343-2352.

52   T. Ahmido, A. Ting and P. Misra, Femtosecond laser-induced breakdown spectroscopy of surface nitrate chemicals, *Appl. Opt.*, 2013, **52**, 3048-3057.

53   T. Delgado, J. M. Vadillo and J. J. Laserna, Laser-induced plasma spectroscopy of organic compounds. Understanding fragmentation processes using ion–photon coincidence measurements, *J. Anal. At. Spectrom.*, 2013, **28**, 1377-1384.

54   S. S. Harilal, C. I. Riju, C. V. Bindhu, V. P. N. Nampoori and C. P. G. Vallabhan, Optical emission studies of C species in laser-produced plasma from carbon, *J. Phys. D: Appl. Phys.,* 1997, **30**, 1703-1709.

55   L. St-Onge, R. Sing, S. B´echard and M. Sabsabi, Carbon emissions following 1:064 µm laser ablation of graphite and organic samples in ambient air, *Appl. Phys. A: Mater. Sci. Process.,* 1999, **69**, S913-S916.

56   A. Portnov, S. Rosenwaks and I. Bar, Identification of organic compounds in ambient air via characteristic emission following laser ablation, *J. Lumin.,* 2003, **102–103**, 408-413.

57   X. Su, X. Cheng, C. Meng and X. Yuan, Quantum chemical study on nitroimidazole, polynitroimidazole and their methyl derivatives, *J. Hazard. Mater.,* 2009, **161**, 551-558.

58   F. C. De Lucia and J. L. Gottfried, Characterization of a Series of Nitrogen-Rich Molecules using Laser Induced Breakdown Spectroscopy, *Prop. Explos. Pyrotech.,* 2010, **35**, 268-277.

59   W. C. Lothrop and G. R. Handrick, The relationship between performance and constitution of pure organic explosive compounds, *Chem. Rev.,* 1949, **44**, 419-445.

60   J.A. Aguilera, C. Aragón, A comparison of the temperatures and electron densities of laser-produced plasmas obtained in air, argon, and helium at atmospheric pressure, *Appl. Phys. A,* 1999, **69,** S475-S478.

61   T.A. Labutin, V.N. Lednev, A.A. Ilyin and A.M. Popov, Femtosecond laser induced breakdown spectroscopy, *J. Anal. At. Spectrom.*, 2016, Advance Article, In Press. DOI: 10.1039/C5JA00301F (critical review).

Species	Emission lines (nm) in femtosecond LIB spectra		Emission lines (nm) in nanosecond LIB spectra	
	Air	**Argon**	**Air**	**Argon**
CN	388.32, 387.12, 386.17, 385.5, 385.11 (Δv=0); 359.05, 358.54, 358.36, 356.04 (Δv=−1); 421.6, 419.66,418.52, 418.01, 416.78, 415.83 (Δv=+1)		388.32, 387.12, 386.15, 385.44, 385.01 (Δv=0); 359.01, 358.57, 358.38 (Δv=−1); 422.67, 421.58, 419.69, 418.06, 416.72, 415.78 (Δv=+1)	
C$_2$	516.52, 512.87 (Δv=0), 473.66, 471.5, 469.67, 468.45, 467.82 (Δv=−1); 563.48, 558.51, 554.04, 545.22, 544.61 (Δv=+1)		516.52, 512.9 (Δv=0); 473.59, 471.49, 469.69, 468.45, 467.84 (Δv=−1); 563.48, 558.51, 554.1(Δv=+1)	
			516.52 observed only in 4-NIm,1,4-DNIm and 2,4-DNIm in argon atmosphere	
NH	336.00	Not observed	336.02	Not observed
C & H	247.86 & 656.24	247.88 & 656.24	247.86 & 656.32	247.86 &656.28
O	777.42	777.41	777.23,777.47 (doublet),777.51	777.23,777.47 (doublet)
N	868.23, 742.41, 744.38, 746.89 (triplet)	868.23	742.41, 744.38, 746.89 (triplet),818.54, 818.84, 821.64, 824.50, 844.7, 863.29, 868.48, 868.69, 870.59, 871.44, 872.13	742.41, 744.38, 746.89 (triplet),
Ca I, II	393.36 (Ca I)	-	393.36 (Ca I), 396.86 (Ca II)	-
Fe I, II	Fe I (306.32, 589.05, 589.64)	-	Fe II (335.98, 354.88, 353.84), Fe I (353.25, 355.56, 394.69, 394.48)	-
Na I, II	Na II (309.98, 309.64, 308.99)	-	Na II (309.98, 309.64, 308.99),, (Na I) (588.99, 589.59)	-
Argon lines (Ar I, II)	-	Ar II (696.61), Ar I (738.52, 750.39, 751.59, 763.72, 772.47, 794.81, 801.68, 811.63, 826.46, 840.93, 842.67)	-	Ar II (696.65), Ar I (738.55, 750.52, 751.62, 763.74, 772.54, 801.65, 810.50, 811.69, 826.67, 840.98, 842.56)

Table 1 Wavelengths of molecular (CN, C$_2$ and NH) and atomic (C, H, N, O, Ca, Na, Fe and Ar) emissions observed in LIB spectra of seven nitroimidazoles in air and argon atmospheres with fs and ns excitations.
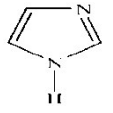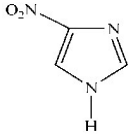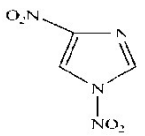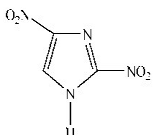
29

Compound	Structure	OB	%C	%H	%N	%O	%C-C	%C=C	% C-N	%C=N
Imidazole ($C_3H_4N_2$)		-188.01	33	44	22	0	0	11	33	11
4-NIm ($C_3H_3N_3O_2$)		-77.83	27	27	27	18	0	9	36	9
1,4-DNIm ($C_3H_2N_4O_4$)		-30.37	23	15	31	31	0	8	31	8
2,4-DNIm ($C_3H_2N_4O_4$)		-30.37	23	15	31	31	0	8	38	8
1M-4NIm ($C_4H_5N_3O_2$)		-107	29	36	21	14	0	7	36	7
2M-4(5)-NIm ($C_4H_5N_3O_2$)		-107	29	36	21	14	7	7	29	7
1M-2,4-DNIm ($C_4H_4N_4O4$)		-55.78	25	25	25	25	0	6	38	6
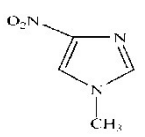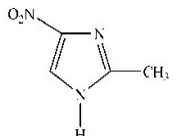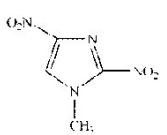
Table 2 OB, % of atoms (C, H, O and N), % of C-C, C=C, C-N and C=N bonds of all nitroimidazoles with their structure and molecular formula.

Sample	Peak	Air (ns)		Argon (ns)	
		fs-LIBS	**ns-LIBS**	**fs-LIBS**	**ns-LIBS**
Im	**CN**	213±28	165±23	1135±15	575±91
	C$_2$	219±47	192±2	**431±18**	876±2
	C	44±3	1186±35	130±36	815±54
1,4-DNIm	**CN**	79±23	2420±150	916±56	926±38
	C$_2$	33±4	342±20	**39±2**	626±3
	C	26±4	854±39	372±29	1171±80
2M-4(5)-NIm /	**CN**	369±120	7128±100	309±91	561±41
1M-4NIm (ns)	**C$_2$**	373±90	496±33	**98±6**	485±13
	C	71±8	1014±66	148±14	667±27

Table 3 Decay times of CN, C$_2$ and C species in Im, 1,4-DNIm, 2M-4(5)-NIm and 1M-4NIm using fs and ns excitations in air and argon atmospheres. CN represents the strongest peak at 388.32 nm, whereas C$_2$ represents the strongest peak at 516.52 nm and C at 247.86 nm.

31

Compound	Bond	BDE(kcal/mol)
4-NIm	C4-NO$_2$	73.5
2,4-DNIm	C2-NO$_2$	69.1
	C4-NO$_2$	70.1
1M-4NIm	C4-NO$_2$	73.9
1M-2,4-DNIm	**C2-NO$_2$**	Data not available
	C4-NO$_2$	

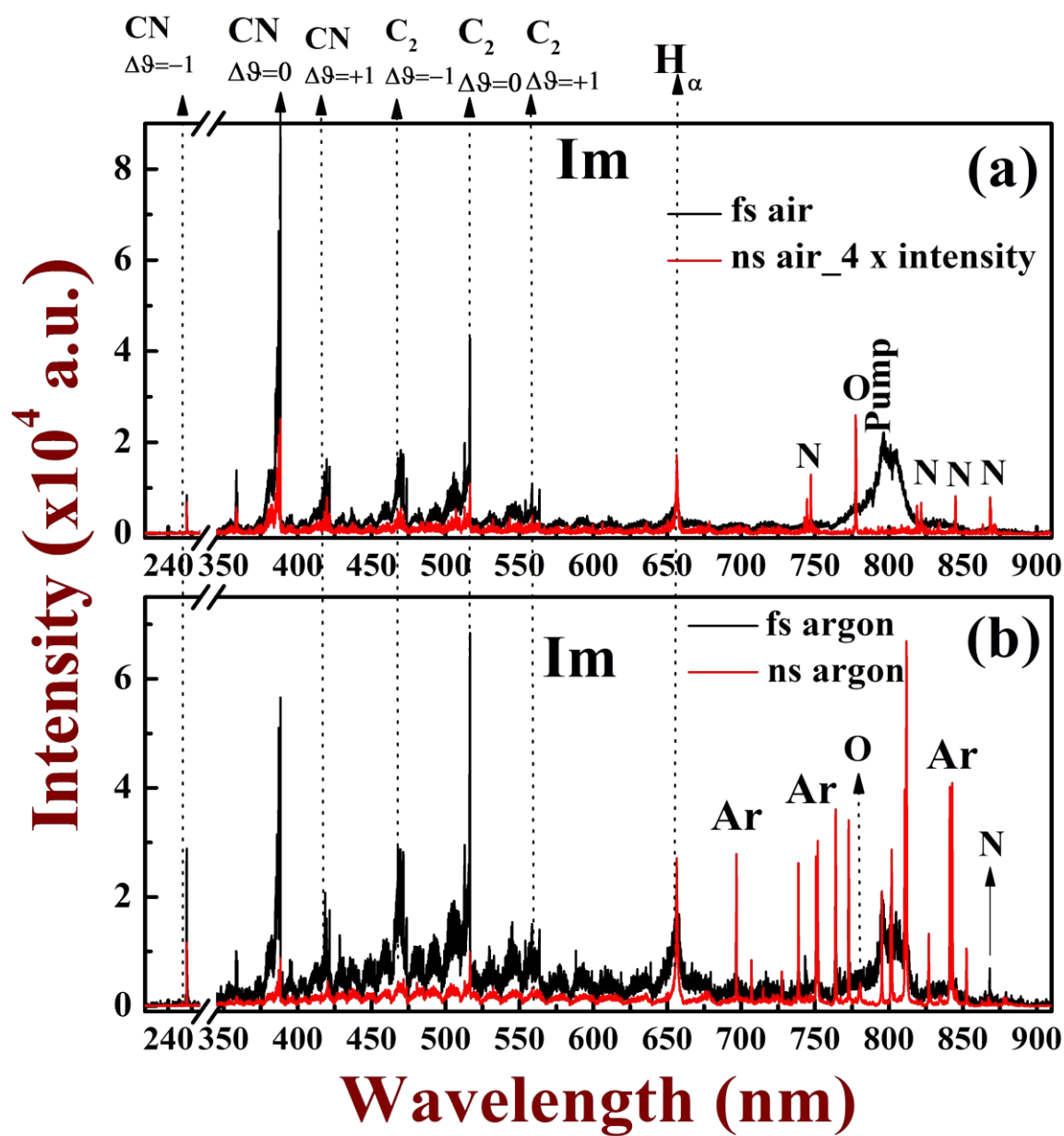**Table 4** C-NO$_2$ bond dissociation energies (BDE); bond highlighted in black is the weakest bond.

Figure 1 Comparison of LIB spectra of imidazole (Im) obtained with fs and ns excitations of (a) air and (b) argon atmospheres. A gate delay of 100 ns, gate width of 800 ns at 1 mJ energy was used in the fs case while in the ns case the delay was 1100 ns, gate width was 10 μs and input pulse energy was ~25 mJ. Each spectrum is a resultant of average of five independent measurements.
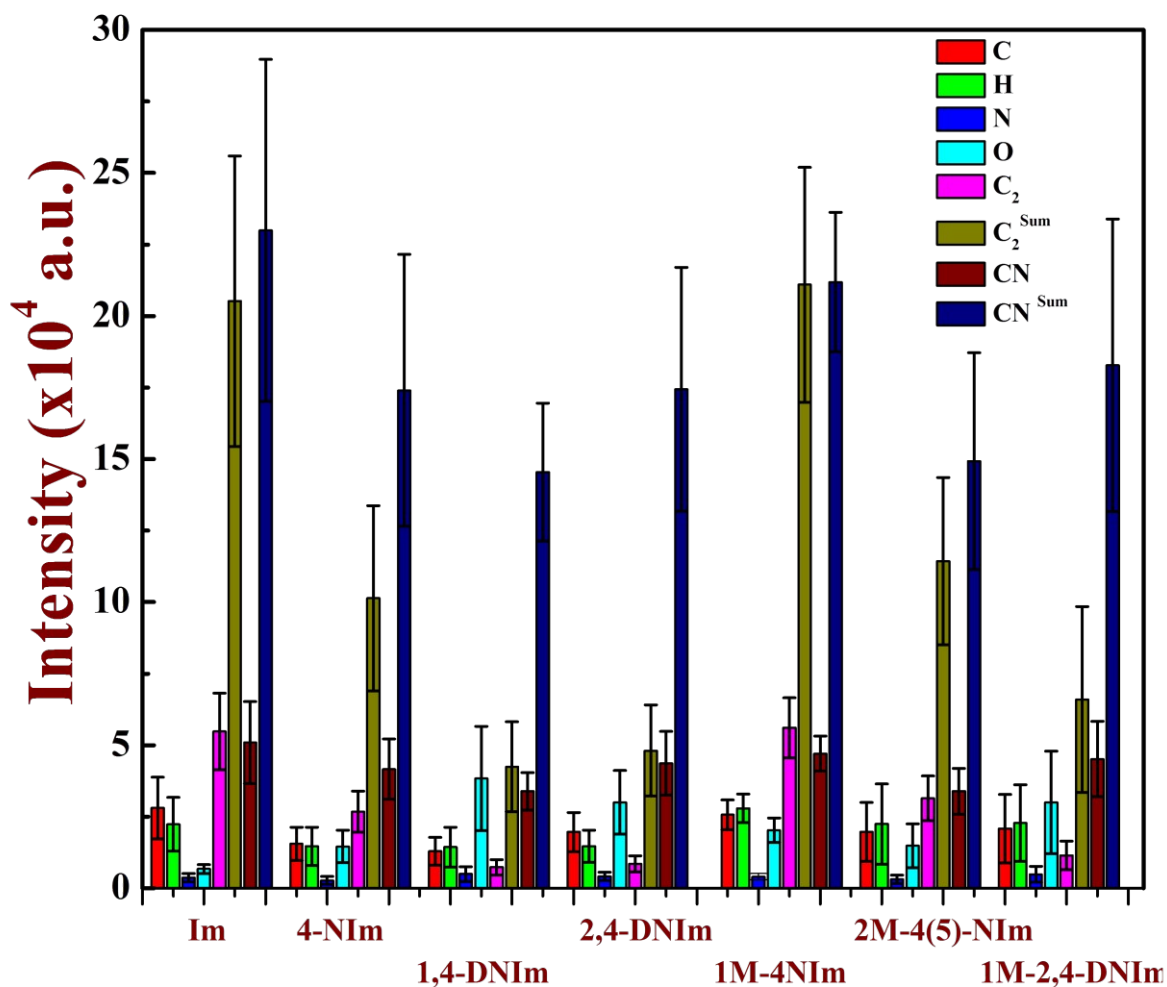
Figure 2 Bar graph of molecular and atomic emission intensities of CN, CN ^{Sum}, C$_2$, C$_2$^{Sum}, C, H$_\alpha$, O and N observed in the fs-LIB spectra of seven nitroimidazoles in argon atmosphere. Each bar chart corresponds to an average intensity of 15 spectral events and the error bar represents standard deviation.
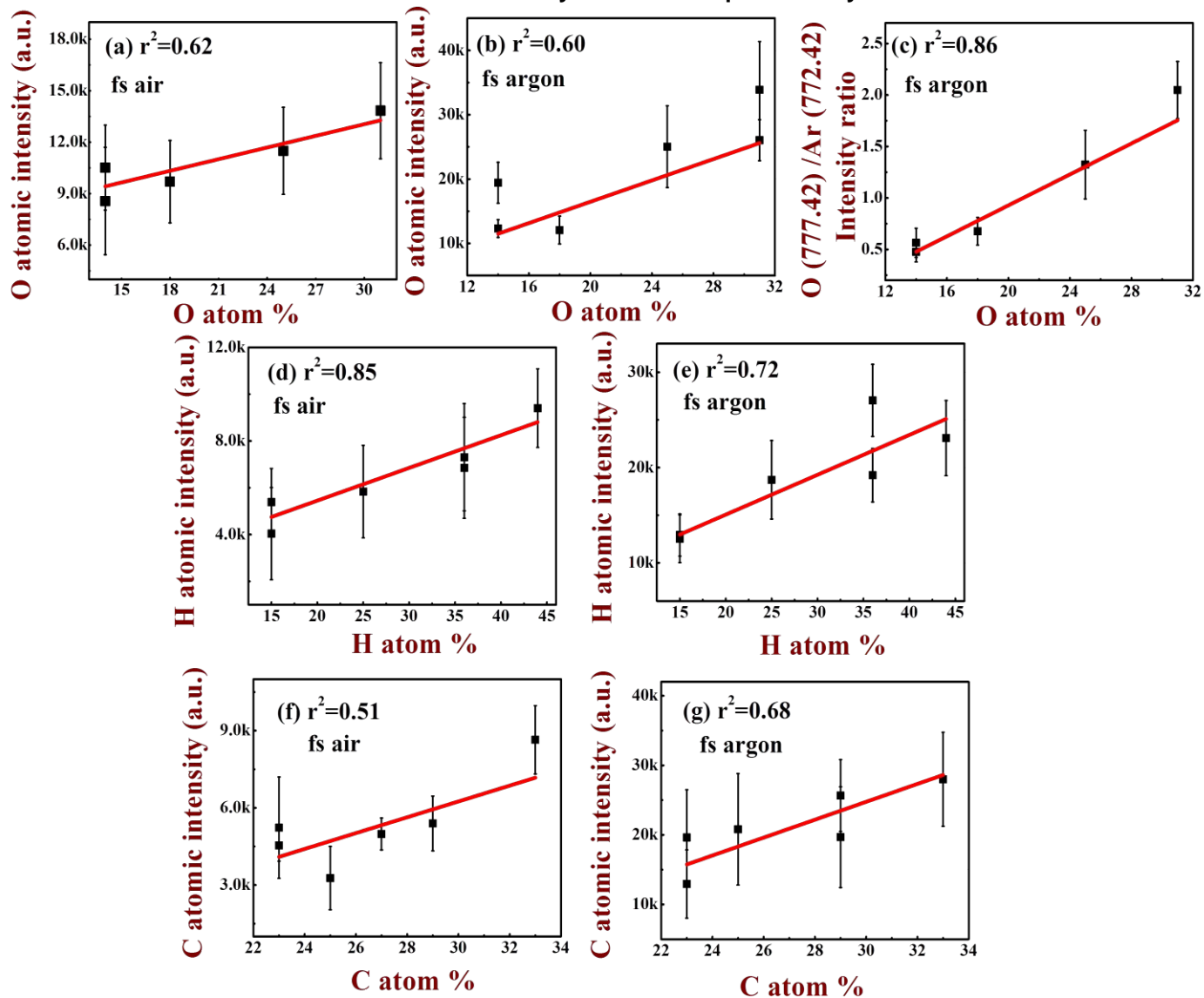
Figure 3 Correlation between O atomic emission intensity in fs-LIB spectra and O atom % in (a) air (b) argon atmosphere (c) O/Ar intensity ratio versus O atom % (ii) H atomic emission intensity versus % H atom in (d) air (e) argon; (iii) correlation between C atom % versus C_2 atomic intensity in (f) air and (g) argon atmospheres. 15 spectra in argon and five spectra in air were used for these calculations.
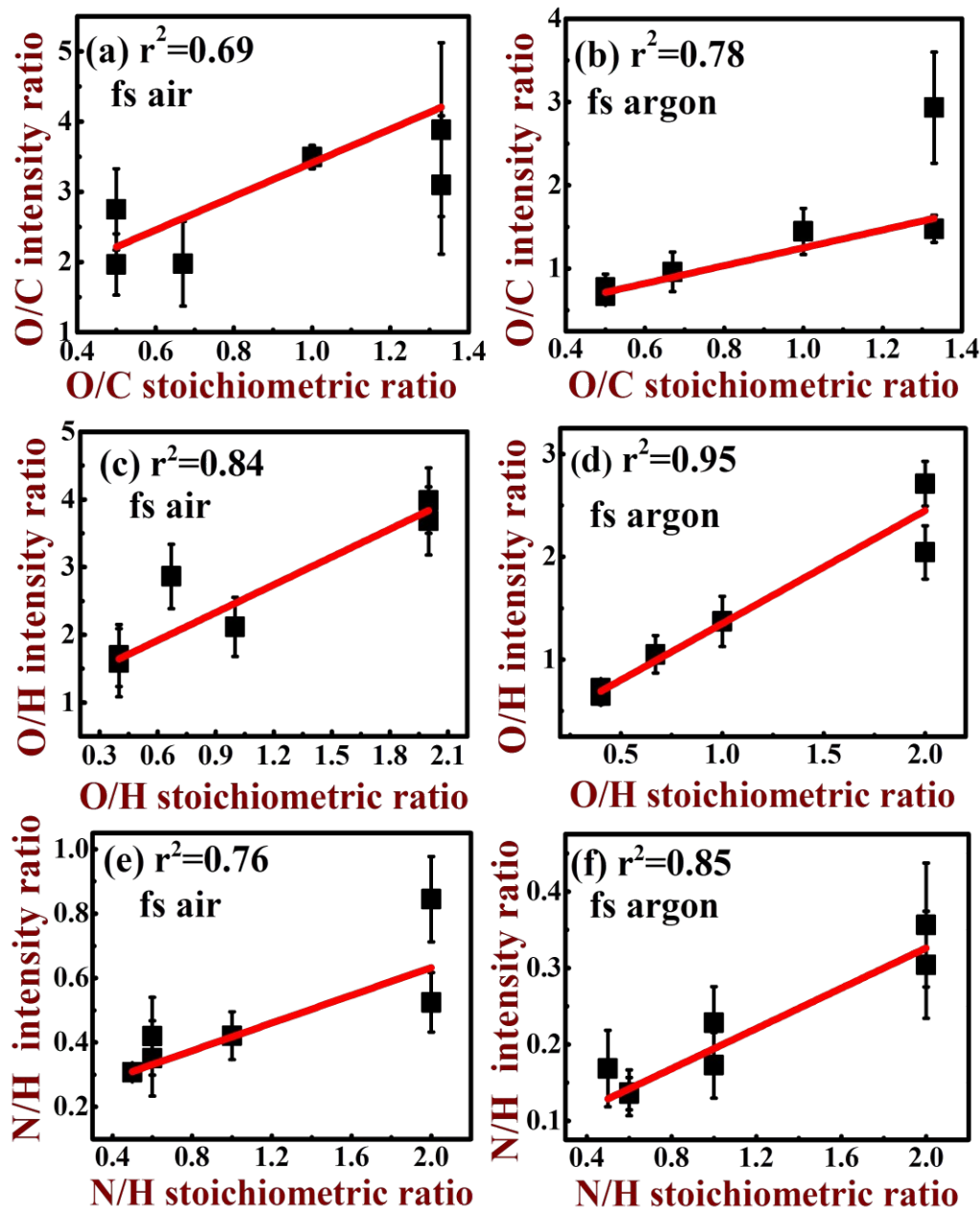
Figure 4 Correlation between **(i)** O/C stoichiometric ratio versus O/C atomic emission ratio correlation for **(a)** fs case air and **(b)** fs case in argon **(ii)** O/H stoichiometric ratio versus O/H atomic emission ratio correlation for **(c)** fs case in air **(d)** fs case in argon and **(iii)** N/H stoichiometric ratio versus N/H atomic emission ratio correlation for **(e)** fs case in air **(f)** fs case in argon atmosphere.
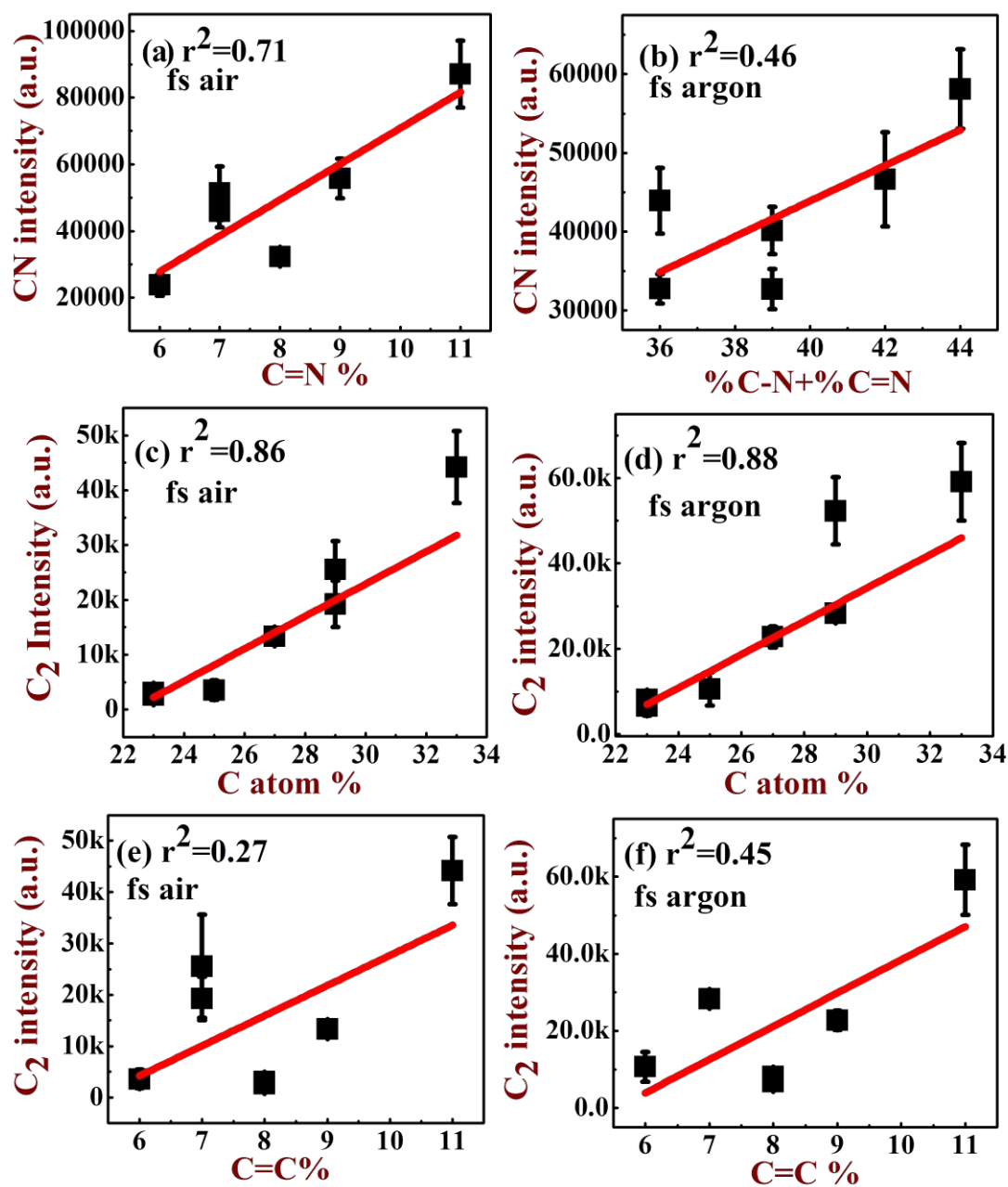
Figure 5 The correlation between the **(i)** CN emission intensity in fs-LIB spectra versus sum of %C=N and sum of %C-N and %C=N in (a) air, (b) argon **(ii)** C_2 versus %C in (c) air, (d) argon **(iii)** C_2 versus %C=C in (e) air, (f) argon.
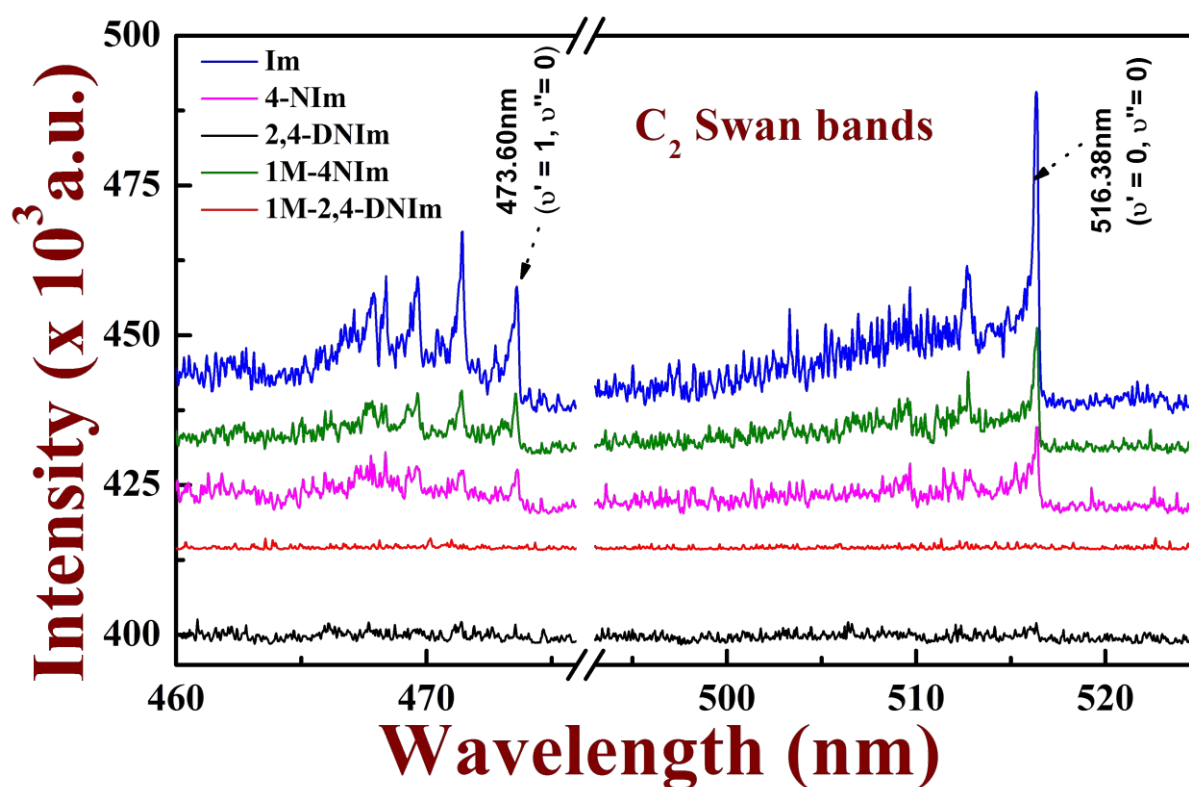
Figure 6 Trend in C_2 Swan band emission intensities for the five imidazole series recorded at a gate delay of 283 ns and gate width of 800 ns with fs excitation in air atmosphere.
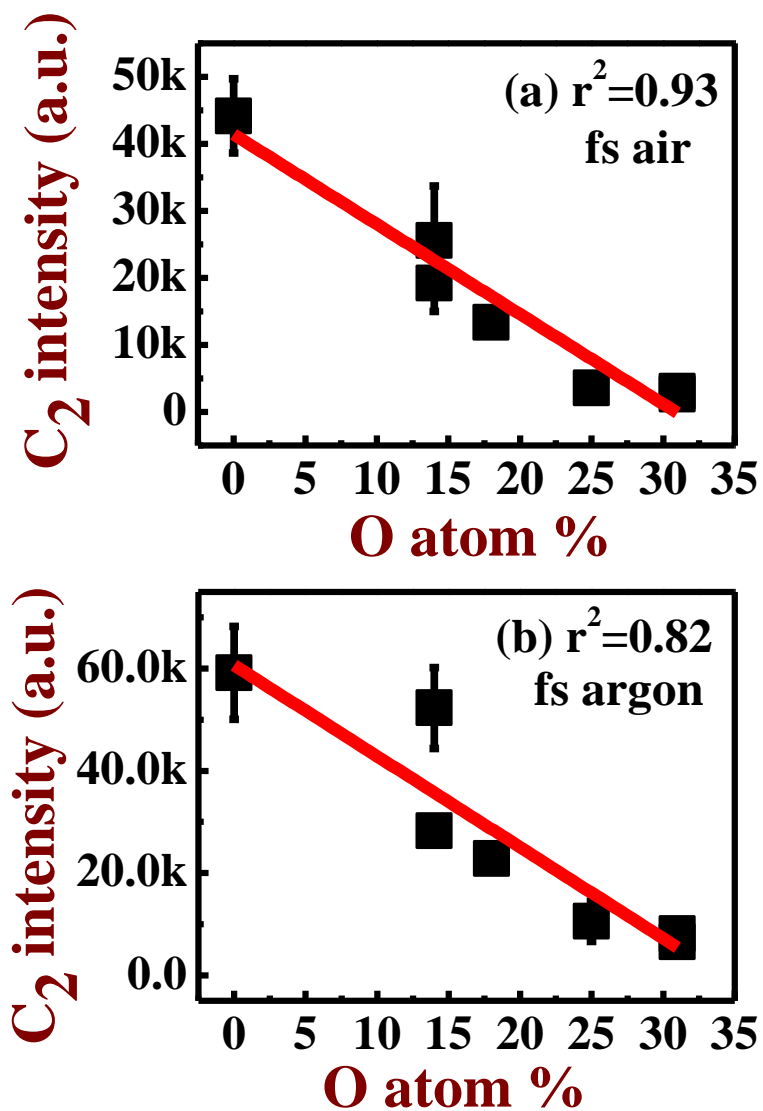
Figure 7 The correlation between the C_2 intensity versus O atom % with fs excitation in **(a)** air and **(b)** argon atmospheres.
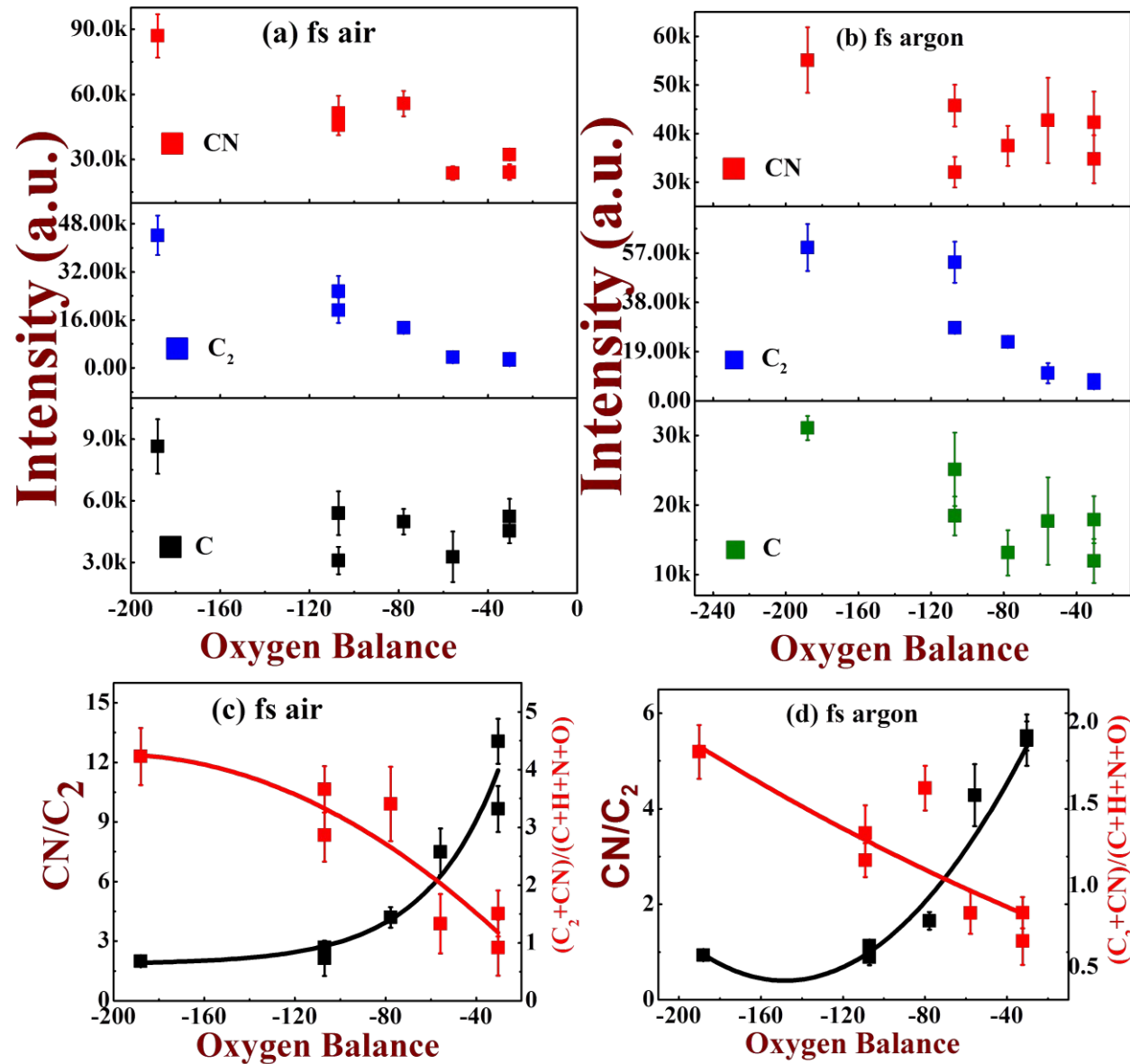
Figure 8 fs-LIB signal emission intensity of molecular bands CN (388.32 nm), C_2 (516.52 nm) and atomic line C (247.86 nm) in **(a)** air, **(b)** argon atmosphere and **(c)** CN/C_2 and (C_2+CN)/(C+H+N+O) versus oxygen balance (OB) in **(c)** air and **(d)** argon atmosphere.
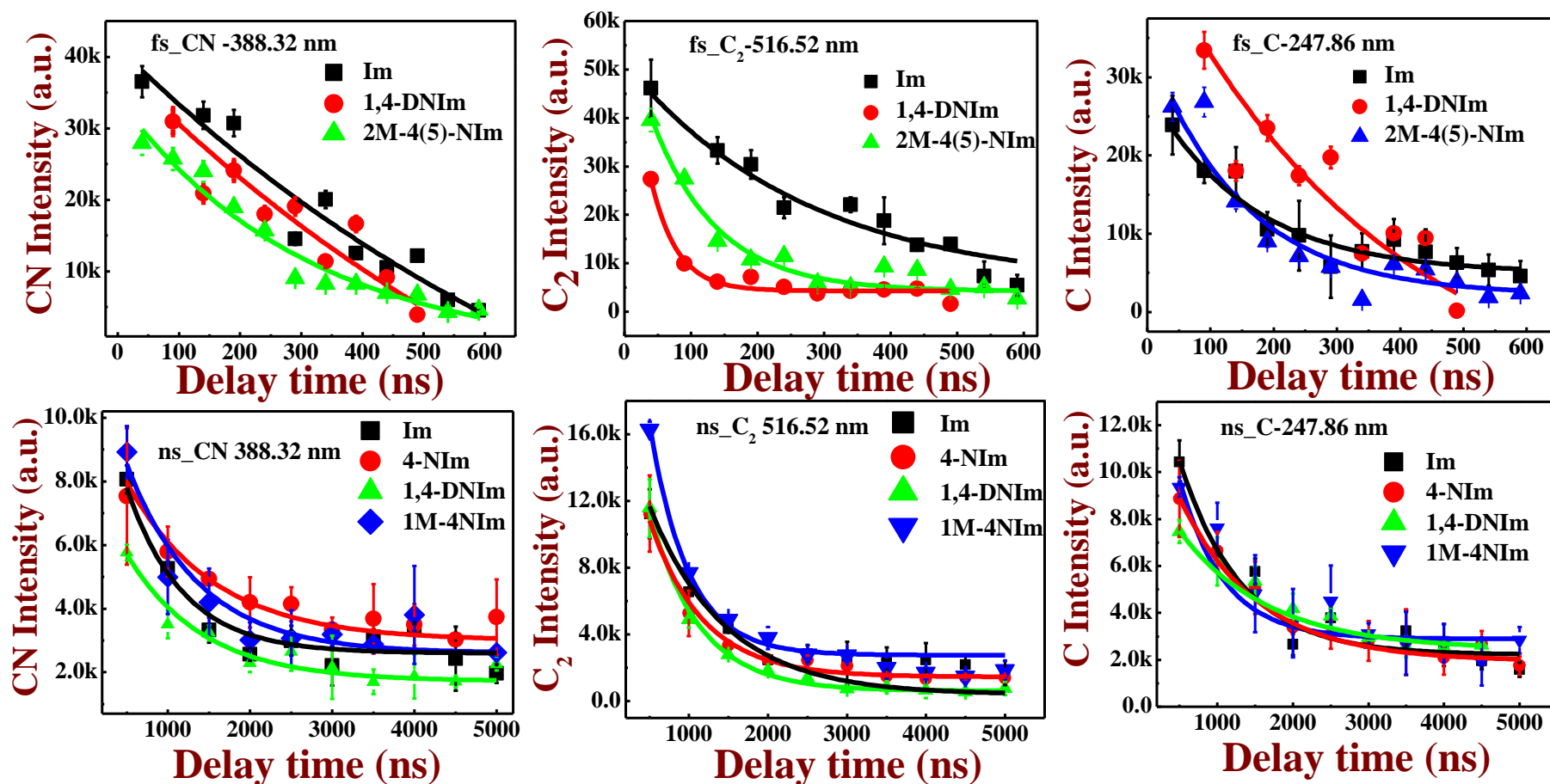
Figure 9 Time resolved emission decays of the molecular bands of the CN (388.32 nm), C_2 (516.52 nm) and C (247.86 nm). A gate delay of 90 ns, gate width of 50 ns were used in fs excitation (argon) while in the ns excitation case a gate delay of 500 ns and a gate width of 500 ns were used in argon atmospheres for Imidazole, 4-NIm, 1,4-DNIm and 2M-4(5)-NIm and 1M-4NIm. Each data point represents the average of three individual measurements and error bars represent the standard deviation of each data point.